

Pentanuclear Cyanide-Bridged Complexes with High Spin Ground States $S = 6$ and 9 : Characterization and Magnetic Properties

Arnaud Marvilliers,* Cédric Hortholary,* Guillaume Rogez,* Jean-Paul Audière,* Eric Rivière,* Joan Cano Boquera,* Carley Paulsen,† Vincent Villar,† and Talal Mallah*¹

*Laboratoire de Chimie Inorganique, UMR CNRS 8613, Université Paris-Sud, 91405 Orsay, France; and †Centre de Recherche sur les Très Basses Températures, CNRS, 25, av. des Martyrs, F-38054 Grenoble, France
E-mail: mallah@icmo.u-psud.fr

Received March 20, 2001; accepted March 21, 2001

IN DEDICATION TO THE LATE PROFESSOR OLIVIER KAHN FOR HIS PIONEERING CONTRIBUTIONS TO THE FIELD OF MOLECULAR MAGNETISM

Two pentanuclear complexes are obtained from the reaction of hexacyanochromate(III) with one to two molar equivalents of $[\text{Ni}(\text{H}_2\text{O})_6]^{2+}$ and bidentate organic ligands that chelate the metal ion, leaving two coordination sites in *cis* positions. Even though the crystal structure was not solved, the full characterization supports the formation of pentanuclear discrete species. $[\text{Cr}(\text{CN})_6]_2[\text{Ni}(\text{HIM2-py})_2]_3 \cdot 7\text{H}_2\text{O}$, **1**, has a ground spin state $S = 6$ owing to the ferromagnetic interaction between Cr^{III} ($S = 3/2$) and Ni^{II} ($S = 1$). The presence of six organic radicals that couple ferromagnetically with Ni^{II} in $[\text{Cr}(\text{CN})_6]_2[\text{Ni}(\text{IM2-py})_2]_3 \cdot 7\text{H}_2\text{O}$, **2**, leads to an $S = 9$ ground state. A.c. susceptibility measurements below 2K indicate the occurrence of an antiferromagnetic order at 1.5 K in **2**. © 2001 Academic Press

Key Words: high spin molecules; cyanide; chromium; nickel; ferromagnetism.

INTRODUCTION

One of the most challenging issues in the field of molecular magnetism (1) is the preparation of magnetic clusters with designed topology and predictable properties. Organic nitroxide-based radicals have been successfully used to design 2D (2), 1D (3), and 0D (4) systems where the radical bridges the metal ions. Recently, pyridine-iminonitroxide radicals were used not as a bridge but as an extra shell of paramagnetic species in order to enhance the spin of the ground state and to prepare a new type of high-spin molecules (5, 6). We report here the preparation, the characterization, and the magnetic properties of two pentanuclear complexes of general formula $[\text{Cr}(\text{CN})_6]_2[\text{Ni}(L)_2]_3 \cdot 7\text{H}_2\text{O}$, where *L* may be the pyridine-iminonitroxide organic radical (IM2-py) or its hydroxylamine derivative (HIM2-py)

Scheme 1). A preliminary report on $[\text{Cr}(\text{CN})_6]_2[\text{Ni}(\text{IM2-py})_2]_3 \cdot 7\text{H}_2\text{O}$ **2** has already been published (5).

EXPERIMENTAL

The IM2-py organic radical and its hydroxylamine derivative have been synthesized by literature procedure (7).

The magnetic data in the temperature range 300–2 K were obtained using a Quantum Design SQUID magnetometer. The low-temperature susceptibility measurements were performed on a homemade SQUID operating in ac (0.001–5000 Hz) and dc modes in the temperature region 4–0.08 K. The magnetization versus the applied magnetic field measurements were carried out at $T = 2$ K using a homemade magnetometer that operates in the field range 0–14 T.

The electronic spectra were registered in solution on a Cary 5E Varian spectrophotometer in the wavelength region 1100–400 nm.

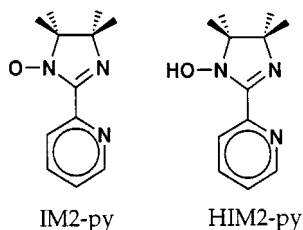
Thermogravimetric and differential thermal analysis were carried out on a homebuilt apparatus under argon between 20 and 230°C at a heating rate of 2°C per minute.

Preparation of Compounds

$[\text{Cr}(\text{CN})_6]_2[\text{Ni}(\text{HIM2-py})_2]_3 \cdot 6.5\text{H}_2\text{O}$, **1**, was prepared under Ar by dissolving $[\text{Ni}(\text{H}_2\text{O})_6](\text{NO}_3)_2$ (10^{-3} mol, 0.291 g) in 50 ml of water to which was added 20 ml of an aqueous solution containing 2×10^{-3} mol (0.562 g) of HIM2-py. The mixture was stirred for a few minutes and then $\text{K}_3[\text{Cr}(\text{CN})_6] \cdot 2\text{H}_2\text{O}$ (6.7×10^{-4} mol, 0.242 g in 20 ml of water) was added dropwise. A precipitate immediately appeared. It was filtered, thoroughly washed with water, and dried under vacuum for 24 h. Elemental analysis: found, C, 49.5; H, 5.67; N, 20.88; Ni, 9.01; Cr, 5.18. Calculated for **1**, C, 49.82; H, 5.74; N, 20.75; Ni, 8.69; Cr, 5.13.

¹ To whom the correspondence should be addressed.





SCHEME 1.

Compound **2** $[\text{Cr}(\text{CN})_6]_2[\text{Ni}(\text{IM2-py})_2]_3 \cdot 7\text{H}_2\text{O}$ **4** was prepared following the same procedure as that for **1**. Elemental analysis: found, C, 49.85; H, 5.32; N, 20.86; Ni, 8.57; Cr, 5.02. Calculated for **2**, C, 49.74; H, 5.46; N, 20.71; Ni, 8.68; Cr, 5.12.

The infrared spectra of **1** and **2** show the bands expected for the organic ligands, in addition to two bands at 2130 and 2170 cm^{-1} , attributed to the asymmetric vibrations of the cyano unit. Furthermore, **1** has a band at 3217 cm^{-1} due to the vibration of the OH group of the hydroxylamine function that is absent in **2**. No bands associated with the nitrate anion are observed in the spectra of **1** and **2** (Fig. 1).

RESULTS AND DISCUSSION

Characterization and Discussion of the Structure

The reaction of hexacyanochromate(III) with $[\text{Ni}(\text{H}_2\text{O})_6]^{2+}$ and HIM2-py led to the formation of a neutral compound as evidenced from the elemental analysis and from the lack of vibration bands associated with the nitrate anion in the infrared spectrum. The infrared spectrum presents in the region 2000–2200 two bands at 2170 and 2130 cm^{-1} that can be attributed the asymmetric vibrations of bridging and nonbridging cyanides. Compound **1** is insoluble in common solvents, which may suggest the formation of an extended structure. However, compound **2** obtained by using the organic radical has the same infrared characteristics and is soluble in common solvents (CH_3OH , CH_2Cl_2 , CHCl_3 ...) and is insoluble in water and ether.

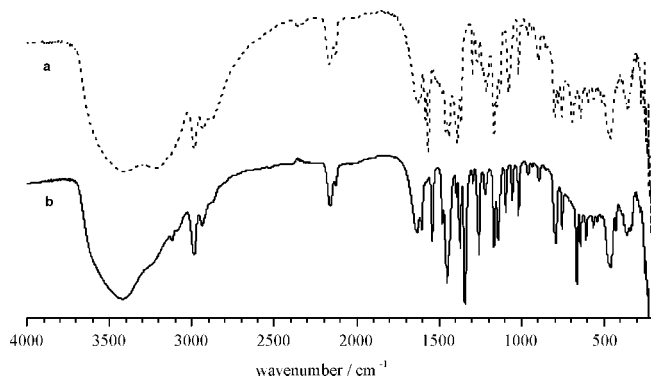


FIG. 1. Infrared spectra in KBr pellet: **1** (a), **2** (b).

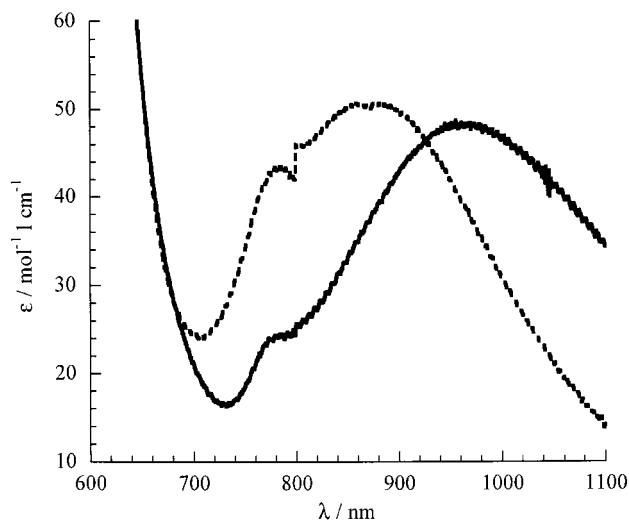
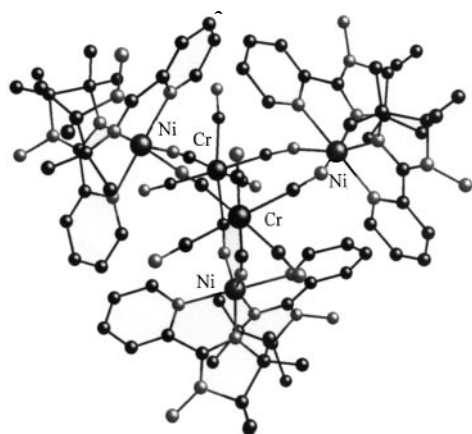


FIG. 2. Electronic spectra: $[\text{Ni}(\text{IM2-py})_2(\text{H}_2\text{O})_2]^{2+}$ (—), **2** (---).

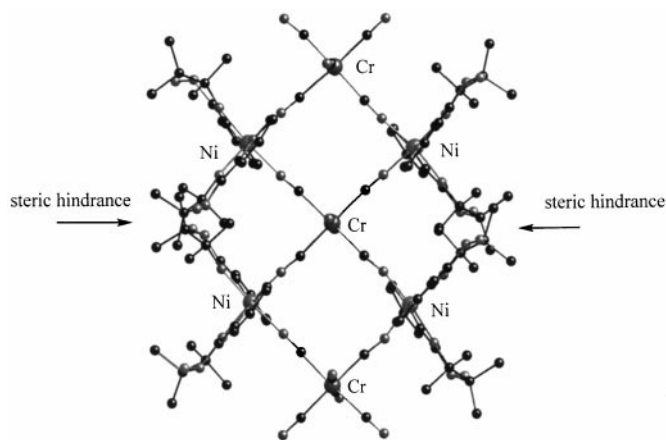
In order to check the nature of the species present in solution when compound **2** is dissolved in methanol (for instance) and particularly to check whether the dissolution is due to the breaking of coordination bonds or just to the solvation of a molecular species already present in the solid state, we registered the UV-visible spectra of a methanolic solution containing a 1 to 2 M equivalent of $[\text{Ni}(\text{H}_2\text{O})_6]^{2+}$ (NO_3)₂ and IM2-py and that of compound **2** in the same solvent (Fig. 2). The spectrum of the $[\text{Ni}(\text{IM2-py})_2(\text{H}_2\text{O})_2]^{2+}$ species presented a large absorption band centered at 957 nm ($\epsilon = 48 \text{ mol}^{-1} \text{ l cm}^{-1}$) assigned to the ${}^3T_{1g} \leftarrow {}^3A_{2g}$ electronic transition, while the band absorption assigned to the same transition in **2** is shifted by 85 nm (1018 cm^{-1}) toward high energy ($\lambda = 872 \text{ nm}$, $\epsilon = 48 \text{ mol}^{-1} \text{ l cm}^{-1}$). If the dissolution of **2** is due to the breaking of an extended structure, the species present in solution must have the same coordination sphere as $[\text{Ni}(\text{IM2-py})_2(\text{H}_2\text{O})_2]^{2+}$ and hence no blue shift could be observed. The only explanation of the observed shift is the presence in the coordination sphere of Ni^{II} of ligands that induce a ligand field larger than that of water (or methanol). These can only be the nitrogen atoms of hexacyanochromate(III) since it has been proven that the cyanide's nitrogen atom induces a ligand field slightly stronger than that of water molecules (8). So the dissolution of compound **2** is probably due to the solvation of a molecular discrete species that already exists in the solid state. If, at this stage, we assume that the two compounds have the same molecular structure (absent of extended coordination bonds), the nonsolubility of **1** may be due to the presence of a hydrogen bonds network that links the molecules together. This is not unreasonable because of the presence of OH groups on the bidentate HIM2-py ligand that are absent in IM2-py. An additional proof to



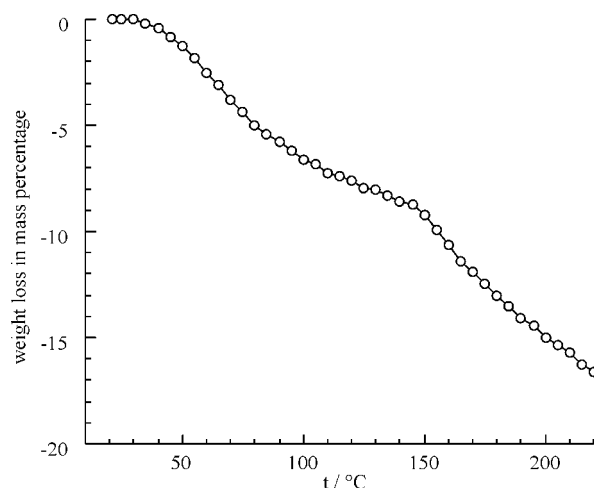
SCHEME 2.

support this hypothesis is given when examining the magnetic properties (see below).

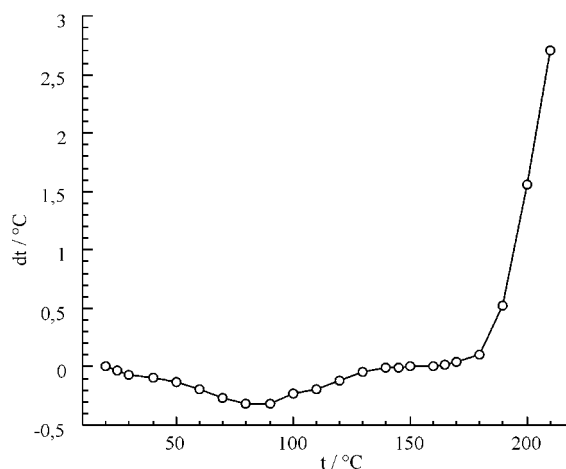
A possible structural model for the discrete species present in compounds **1** and **2** is given in Scheme 2. It consists of a pentanuclear neutral complex where three $\text{Ni}(\text{L})_2$ species bridge two $\text{Cr}(\text{CN})_6$ molecules. This structural model contains all the characteristics expected for compounds **1** and **2**: (i) the availability of two coordination sites in the $\text{Ni}(\text{L})_2$ species in *cis* position, (ii) the presence of bridging and non-bridging cyanide groups, (iii) the Ni/Cr ratio equal to $\frac{3}{2}$, which leads to neutral compounds, and more importantly (iv) the bulkiness of the bidentate ligands that preclude the formation of an extended system as presented in Scheme 3 where we show two Cr_2Ni_2 squares sharing one chromium vertex. The steric hindrance appears to be due to the methyl groups of the ligands. An extended 1D system based on Cr_2M_2 squares sharing chromium vertices is possible with less bulky ligands like bispicen as we have reported for $[\text{Cr}(\text{CN})_6]_3[\text{Mn}(\text{bispicen})]_2 \cdot 6\text{H}_2\text{O} \cdot 0.5\text{C}_2\text{H}_5\text{OH}$ (**9**) (bispicen is a tetradentate ligand that leaves two coordination sites in *cis* position on manganese).



SCHEME 3.

FIG. 3. Thermogravimetric analysis for **1**.

Thermogravimetric analysis (TGA) of compound **1** (Fig. 3) is consistent with the loss of seven water molecules between 20 and 140°C, which corresponds to the endothermic transformation observed in the differentialthermo analysis (DTA) plot (Fig. 4). Above 150°C, the exothermic transformation in the DTA plot indicates the formation of new bonds probably as the result of a rearrangement within the compound due to decomposition. The corresponding mass loss in the TGA plot cannot be due to that of water molecules. Indeed, the infrared spectrum of a sample heated at 140°C is identical to that of a nonheated sample, while the spectra of two samples heated at 170 and 210°C show a complete change in the bands corresponding to the organic ligand and to cyanides. This is in line with the decomposition that occurs when the temperature exceeds 150°C.

FIG. 4. Differentialthermal analysis for **1**.

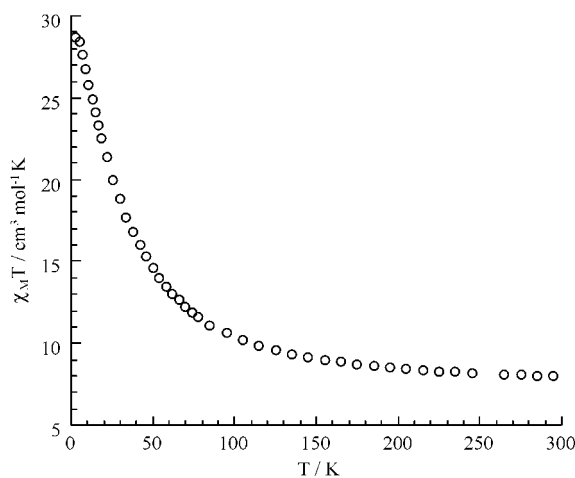


FIG. 5. Thermal variation of the susceptibility times the temperature in the form of $\chi_M T$ versus T plot for **1**.

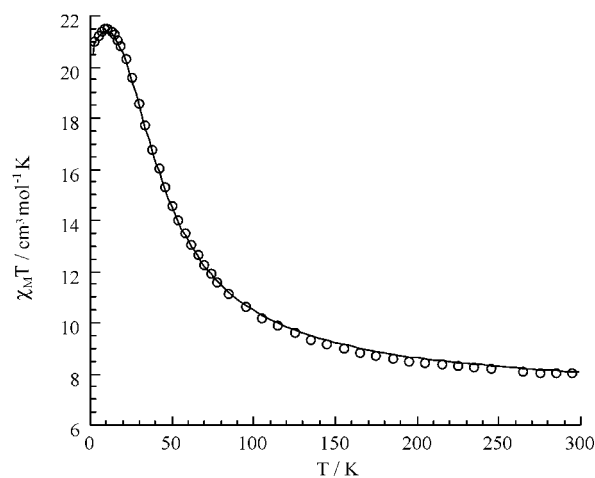


FIG. 6. Thermal variation of the susceptibility times the temperature in the form of $\chi_M T$ versus T plot for a dehydrated sample of **1**: (O) experimental, (—) best fit.

Magnetic Studies: Compound **1**

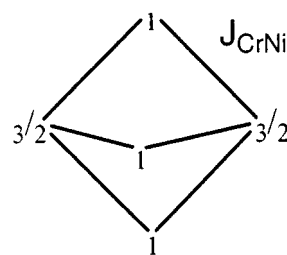
The susceptibility *vs.* temperature measurements performed within an applied magnetic field of 1000 Oe shows that $\chi_M T$ increases on cooling, indicating the occurrence of a ferromagnetic interaction (Fig. 5). The ferromagnetic interaction is expected for a Cr^{III}-CN-Ni^{II} linkage and is due to the orthogonality of the magnetic orbitals (10). The $\chi_M T$ value at room temperature ($7.96 \text{ cm}^3 \text{ mol}^{-1} \text{ K}$) is well above the value corresponding to isolated two Cr^{III} and three Ni^{II} ions ($7.51 \text{ cm}^3 \text{ mol}^{-1} \text{ K}$) when assuming $g_{\text{Ni}} = 2.25$ and $g_{\text{Cr}} = 1.99$. At low temperature (3 K), $\chi_M T$ is found equal to $28.7 \text{ cm}^3 \text{ mol}^{-1} \text{ K}$. This is a much higher value than one may expect for a $S = 6$ ground state resulting from the ferromagnetic interaction within the assumed pentanuclear structure. In such a case, the expected $\chi_M T$ value at low temperature should be equal to $23 \text{ cm}^3 \text{ mol}^{-1} \text{ K}$ (assuming $g_{\text{Cr}} = 1.99$ and $g_{\text{Ni}} = 2.25$). Two possible explanations may be imagined: (i) compound **1** does not contain discrete species but an extended coordination network, and (ii) pentanuclear discrete species are present but they are interacting at low temperature in a ferromagnetic manner. The second explanation is reasonable if we assume, as suggested above, the presence of an H-bonds network linking the discrete species together, making the compound insoluble and favoring intermolecular interactions. Murray and co-workers have actually reported an example of a pentanuclear Fe^{II}Ni^{II}₃ cyanide-bridged complex that orders ferromagnetically due to intermolecular ferromagnetic interactions at low temperature (11).

In order to check our assumption on the presence of a hydrogen bonds network responsible of the magnetic behavior at low temperature, we carried out a dehydration of compound **1**. The dehydration was done by heating a 30-mg sample under vacuum for 24 h at 140°C. The

dehydrated sample was loaded in the container that is used for the magnetization measurements in a glove box. The $\chi_M T = f(T)$ plot of the dehydrated sample (Fig. 6) is identical to that of **1** in the temperature range, 300–30 K. Below $T = 30 \text{ K}$, the $\chi_M T$ value for the dehydrated sample does not increase as quickly as that of **1**. A maximum of $\chi_M T$ ($21.5 \text{ cm}^3 \text{ mol}^{-1} \text{ K}$) is observed at $T = 9 \text{ K}$. This $\chi_M T$ value corresponds well to what is expected for an $S = 6$ ground state, showing that the intermolecular interactions have been suppressed at least to a certain extent. The decrease of $\chi_M T$ below 9 K may be safely attributed to zero field splitting within the $S = 6$ ground state. The $\chi_M T = f(T)$ data were fitted assuming the coupling scheme (Scheme 4) corresponding to the structural model proposed above. The spin Hamiltonian in zero field is

$$H = -J_{\text{CrNi}}(\mathbf{S}_{\text{Ni}1} \cdot \mathbf{S}_{\text{Cr}1} + \mathbf{S}_{\text{Ni}1} \cdot \mathbf{S}_{\text{Cr}2} + \mathbf{S}_{\text{Ni}2} \cdot \mathbf{S}_{\text{Cr}1} + \mathbf{S}_{\text{Ni}2} \cdot \mathbf{S}_{\text{Cr}2} + \mathbf{S}_{\text{Ni}3} \cdot \mathbf{S}_{\text{Cr}1} + \mathbf{S}_{\text{Ni}3} \cdot \mathbf{S}_{\text{Cr}2}),$$

where J_{CrNi} is the exchange coupling interaction between Cr^{III} and Ni^{II}, and \mathbf{S}_{Ni} and \mathbf{S}_{Cr} are the local spin operators for Ni^{II} and Cr^{III} respectively. The Ni–Ni and Cr–Cr interactions have been neglected. Zero field splitting was introduced only within the ground $S = 6$ state. The $g_{s,s'}$ expression



SCHEME 4.

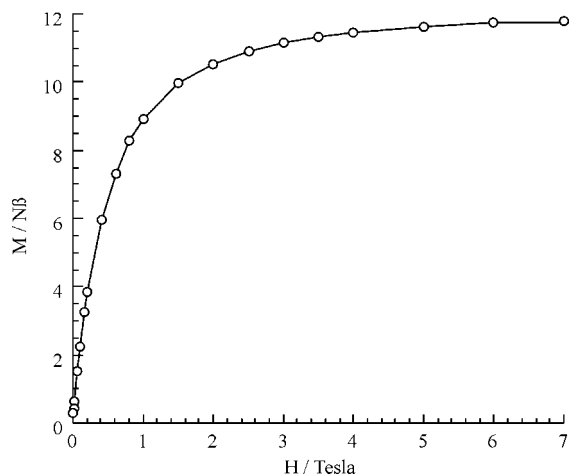


FIG. 7. Variation of the magnetization versus the applied magnetic field in the form $M/N\beta = f(H)$ plot at $T = 3$ K for **1**.

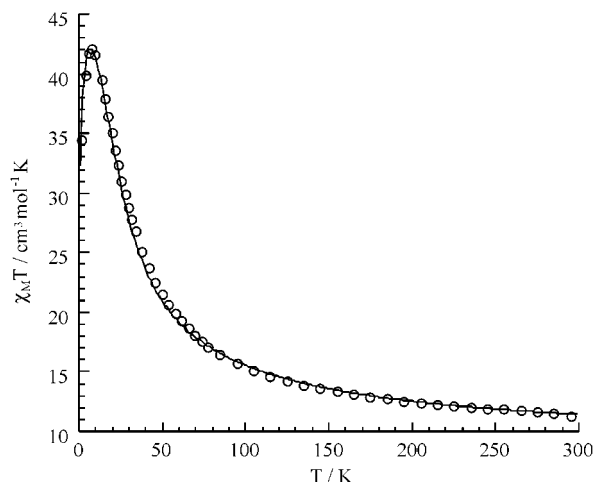


FIG. 8. Thermal variation of the susceptibility times the temperature in the form of $\chi_M T$ versus T plot for **2**: (O) experimental, (—) best fit.

were calculated for each spin state as a function of the local g -factors, g_{Ni} and g_{Cr} (S is the total spin value for each state, and S' and S'' are the intermediate spin values obtained from the summation vector couplings $\mathbf{S}_{\text{Ni}1} + \mathbf{S}_{\text{Ni}2} + \mathbf{S}_{\text{Ni}3}$ and $\mathbf{S}_{\text{Cr}1} + \mathbf{S}_{\text{Cr}2}$, respectively). The susceptibility expression was taken as the average of the parallel and the perpendicular components and was used to fit the experimental data. Because of the presence of four parameters J_{CrNi} , g_{Ni} , g_{Cr} , and D_{GS} , the fit was done several times by each time fixing one parameter value. The best fit, shown in Fig. 6, corresponds to the following values: $J_{\text{CrNi}} = 13.5 \text{ cm}^{-1}$, $g_{\text{Cr}} = 1.99$, $g_{\text{Ni}} = 2.08$, and $D_{\text{GS}} = 0.007 \text{ cm}^{-1}$. The agreement factor was found to be equal to 6.7×10^{-5} .

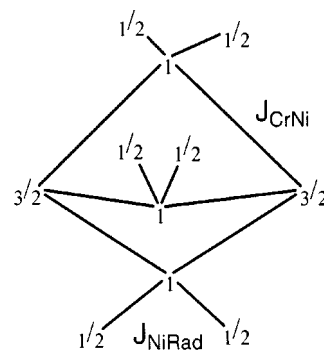
The J_{CrNi} value corresponds well to the expected exchange coupling parameter between Cr^{III} and Ni^{II} bridged by a cyanide group. A value of 15 cm^{-1} was found for the heptanuclear complex $\text{Cr}^{\text{III}}\text{Ni}^{\text{II}}_6$ (10). The high quality of the fitting is a good argument for the validity of the coupling scheme we assumed and thus to our hypothesis of the pentanuclear species structure. It is important to note here that our structural model is the same as the structure of the pentanuclear complex reported by Murray and co-workers (11) and that of the very similar compound reported recently by Rey and co-workers (6).

Magnetization field measurements performed at $T = 3$ K (Fig. 7) is consistent with a spin ground state $S = 6$ since at $H = 7$ T, the saturation value is equal to 12 bohr magnetons.

Magnetic Studies: Compound **2**

The magnetic behavior of compound **2** is similar to that of **1** (Fig. 8), $\chi_M T$ increases on cooling and reaches a maximum value of $42.2 \text{ cm}^3 \text{ mol}^{-1} \text{ K}$ at $T = 7$ K and then decreases. The $\chi_M T$ value at room temperature

($11.18 \text{ cm}^3 \text{ mol}^{-1} \text{ K}$) is well above the expected value for noninteracting six $S = \frac{1}{2}$ radicals, three $S = 1\text{Ni}^{\text{II}}$ and two $S = \frac{3}{2}\text{Cr}^{\text{III}}$ ions ($9 \text{ cm}^3 \text{ mol}^{-1} \text{ K}$ assuming all g values equal 2). If the exchange coupling interaction between Cr^{III} and Ni^{II} is the same as for **1** and if we assume that at room temperature the Ni^{II} and the two chelating organic radicals are not interacting, the $\chi_M T$ value should be equal to 7.96 (this is the $\chi_M T$ value for **1** at room temperature) $+ 6 \times 0.375 = 10.21 \text{ cm}^3 \text{ mol}^{-1} \text{ K}$. The fact that at room temperature $\chi_M T$ is greater than this value indicates the presence of a rather large *ferromagnetic* interaction between Ni^{II} and the iminonitroxide radical. Rey and co-workers have already demonstrated that this is actually the case because of the orthogonality between the π -type magnetic orbital of the radical and the σ -type ($d_{x^2-y^2}$ or d_{z^2}) magnetic orbitals of Ni^{II} in $\text{Ni}(\text{hfac})_2(\text{IM}2\text{-py})$. The J_{NiRad} exchange coupling parameter was found equal to 128 cm^{-1} (12). The coupling scheme (Scheme 5) for compound **2** does not make it possible to establish a theoretical expression for the susceptibility as for **1**. The only way to fit the experimental data is to diagonalize the 27648×27648 energy matrix. The



SCHEME 5.

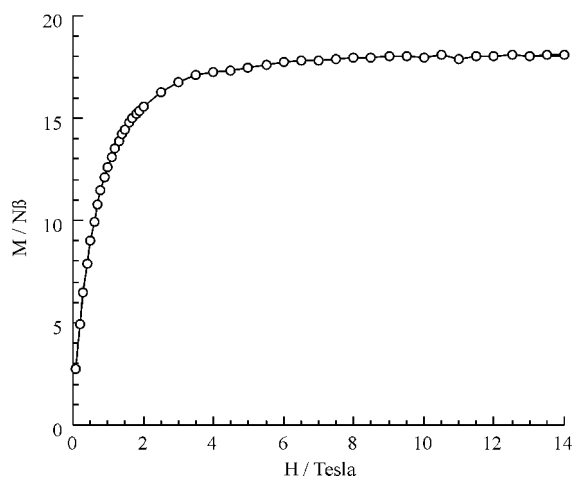


FIG. 9. Variation of the magnetization versus the applied magnetic field in the form $M/N\beta = f(H)$ plot at $T = 2$ K for **2**.

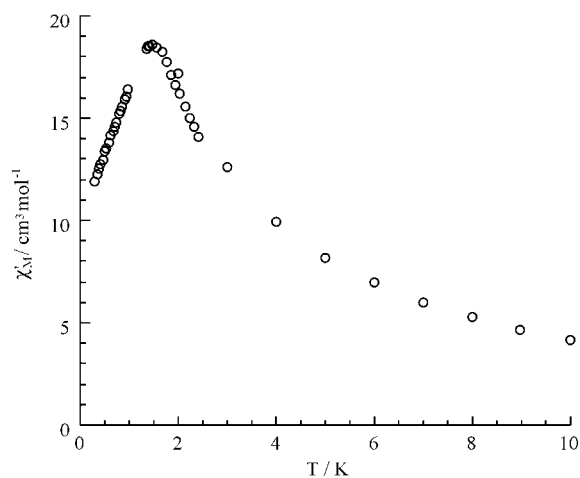


FIG. 10. Thermal variation of the real susceptibility in the form of χ'_M versus T plot for **2** with zero applied dc field and an oscillating ac field of 37 Hz.

susceptibility has been calculated using the fluctuation of the magnetization M , which is calculated from the energy eigenvalues and spin eigenfunctions. The eigensystem solution has been achieved by diagonalizing the energy matrix. The energy matrix is formed of blocks built from the spin function basis in the M_S subspaces, where M_S is the z component of the spin quantum number S . In our case, the size of the bigger block-matrix that must be diagonalized, which corresponds to the $M_S = 0$ subspace, is 4390×4390 . The calculation of $\chi_M T$ was performed for different values of the couple (J_{CrNi} , J_{NiRad}) close the expected values for these parameters. The best agreement was found for $J_{CrNi} = 9 \text{ cm}^{-1}$ and $J_{NiRad} = 105 \text{ cm}^{-1}$. It was possible to introduce an intermolecular interaction parameter θ in order to describe the decrease of $\chi_M T$ below 7 K; a value of -0.45 K was found expressing an intermolecular antiferromagnetic interaction (Fig. 8).

The susceptibility data are thus consistent with the stabilization of a $S = 9$ spin ground state within the pentanuclear species. Magnetization as a function of the applied field performed at $T = 2 \text{ K}$ up to 14 T (Fig. 9) shows a saturation value of 18 bohr magnetons, confirming the $S = 9$ ground state for **2**.

In order to check the possibility of the presence of an antiferromagnetic intermolecular interactions at low temperature, ac susceptibility studies were performed down to 100 mK at two different frequencies (1 and 37 Hz) of the oscillating field in zero applied dc magnetic field. A maximum of the real susceptibility is observed at $T = 1.5 \text{ K}$, but the temperature of the maximum is not frequency

dependent (Fig. 10). This suggests the onset of an antiferromagnetic order at $T = 1.5 \text{ K}$ as a result of the intermolecular antiferromagnetic interaction between the clusters. It was unfortunately impossible to suppress the intermolecular interactions in **2** as was done for compound **1**.

REFERENCES

- O. Kahn, "Molecular Magnetism." VCH, New York, 1994.
- K. Fegy, D. Luneau, T. Ohm, C. Paulsen, and P. Rey, *Angew. Chem. Int. Engl. Ed.* **37**, 1270–1272 (1998).
- A. Caneschi, D. Gatteschi, and P. Rey, *Prog. Inorg. Chem.* **39**, 331–429 (1991).
- A. Caneschi, D. Gatteschi, J. Laugier, P. Rey, R. Sessoli, and C. Zanchini, *J. Am. Chem. Soc.* **110**, 2795–2799 (1988).
- A. Marvilliers, Y. Pei, J. Cano Boquera, K. E. Vostrikova, C. Paulsen, E. Rivière, J.-P. Audière, and T. Mallah, *Chem. Commun.* 1951–1952 (1999).
- K. Vostrikova, D. Luneau, W. Wernsdorfer, P. Rey, and M. Verdager, *J. Am. Chem. Soc.* **122**, 718–719 (2000).
- J. N. Helbert, P. W. Kopf, E. H. Poindexter, and B. E. Wagner, *J. Chem. Soc., Dalton Trans.* 998–1003 (1975).
- D. F. Shriver, S. A. Shriver, and S. E. Anderson, *Inorg. Chem.* **4**, 725–730 (1965).
- A. Marvilliers, S. Parsons, E. Rivière, J.-P. Audière, and T. Mallah, *Chem. Commun.* 2217–2218 (1999).
- T. Mallah, C. Auberger, M. Verdager, and P. Veillet, *J. Chem. Soc. Chem. Comm.* 61–62 (1995).
- K. V. Langenberg, S. R. Batten, K. J. Berry, D. C. R. Hockless, B. Moubarak, and K. S. Murray, *Inorg. Chem.* **36**, 5006–5015 (1997).
- D. Luneau, P. Rey, J. Laugier, E. Belorizky, and A. Cogne, *J. Am. Chem. Soc.* **31**, 3578–3584 (1992).